Electronic Supplementary Information for

A Useful Preparation of Ultrasmall Iron Oxide Particles by using Arc Plasma Deposition

Yumi Ida,[a] Atsushi Okazawa,[b,††] Kazutaka Sonobe,[c] Hisanori Muramatsu,[c] Tetsuya Kambe,[a,c]

Takane Imaoka,[a,c] Wang-Jae Chun,[d] Makoto Tanabe,[a,*] and Kimihisa Yamamoto[a,c,*]

[a]*JST–ERATO, Yamamoto Atom Hybrid Project, Tokyo Institute of Technology, Yokohama 226-8503, Japan.*

[b]*Department of Basic Science, Graduate School of Arts and Sciences, The University of Tokyo, Tokyo 153-8902, Japan.*

[c]*Laboratory for Chemistry and Life Science, Tokyo Institute of Technology, Yokohama 226-8503, Japan.*

[d]*Graduate School of Arts and Sciences, International Christian University, Mitaka, Tokyo 181-8585, Japan.*

[††]*Present address: Division of Chemistry, Institute of Liberal Education, Nihon University School of Medicine, Tokyo 173-8610, Japan.*

Table of Contents:

Table S1. Ratio of the shot count to the weight of the carbon supports.

Sample	Shot count	Weight /g	Ratio (Shot count/g)
KB_{200}	200	0.09815	2038
KB_{400}	400	0.09212	4342
KB_{800}	800	0.1001	7992
KB_{2000}	20000	0.09521	21006
GO_{134}	134	0.3312	405
GO_{267}	267	0.318	840
GO_{534}	534	0.326	1638
GO_{1068}	1068	0.3146	3395
GNP_{3666}	3666	2.26	1622
GNP_{7494}	7494	2.31	3244
GNP_{10900}	10900	2.55	4275
GNP_{18409}	18409	2.44	7545

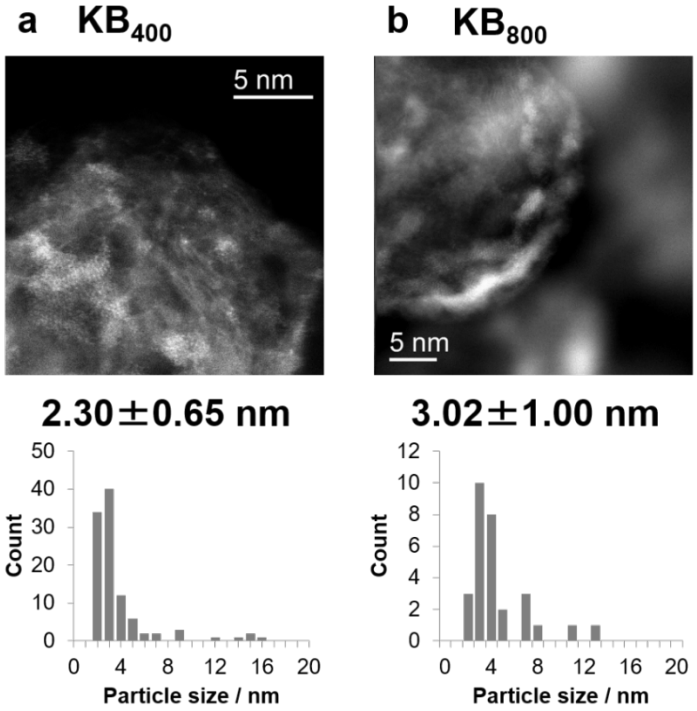

Figure S1. HAADF-STEM images and particle size distribution histograms of a) KB_{400} and b) KB_{800}.

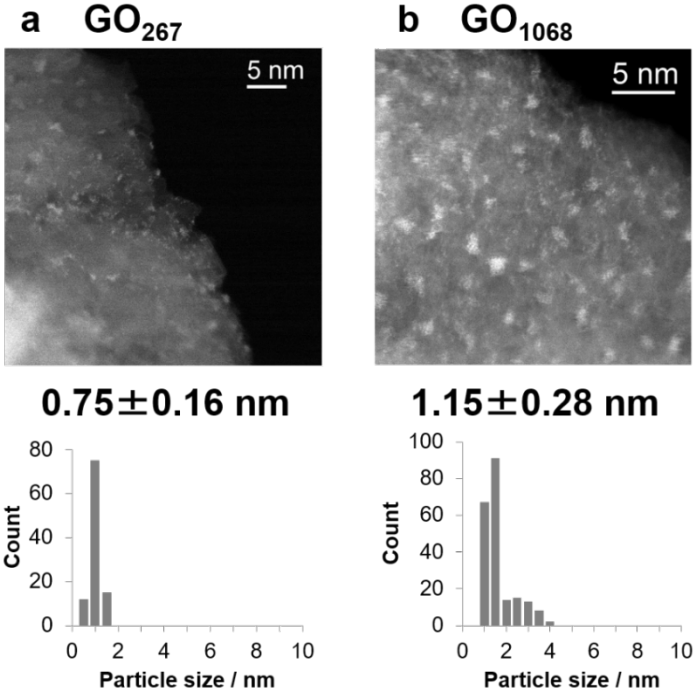

Figure S2. HAADF-STEM images and particle size distribution histograms of a) GO_{267} and b) GO_{1068}.

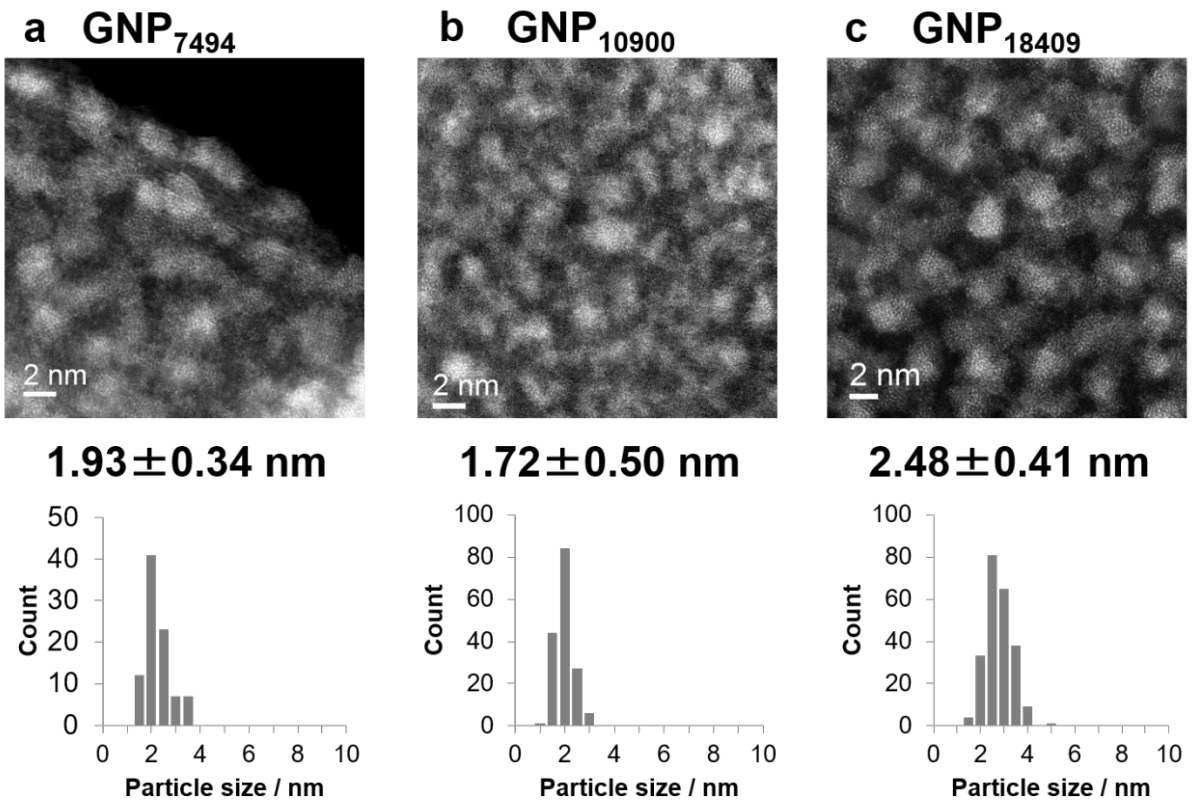

Figure S3. HAADF-STEM images and particle size distribution histograms of a) GNP_{7494}, b) GNP_{10900}, and c) GNP_{18409}.

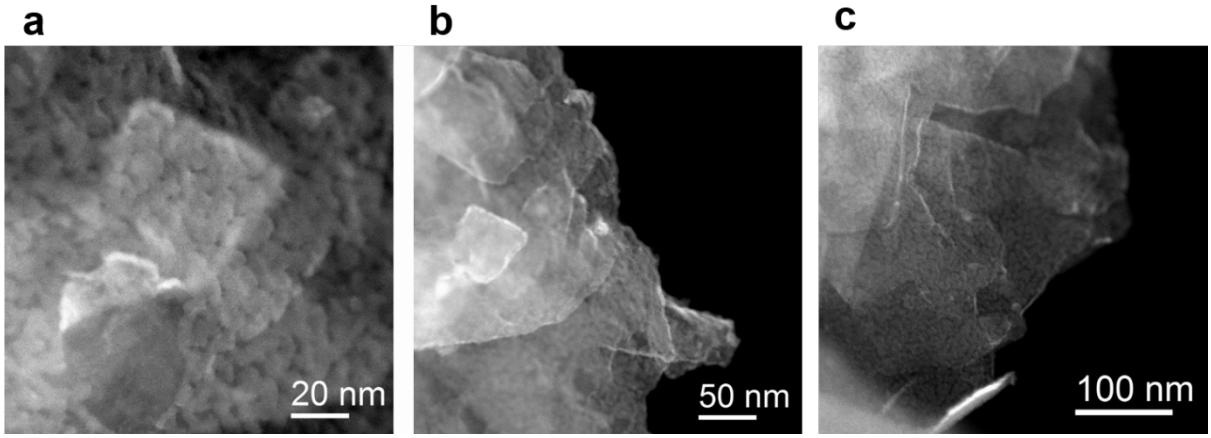

Figure S4. HAADF-STEM images of GNP_{20000} with three different scale bars; a) 20 nm, b) 50 nm, and c) 100 nm.

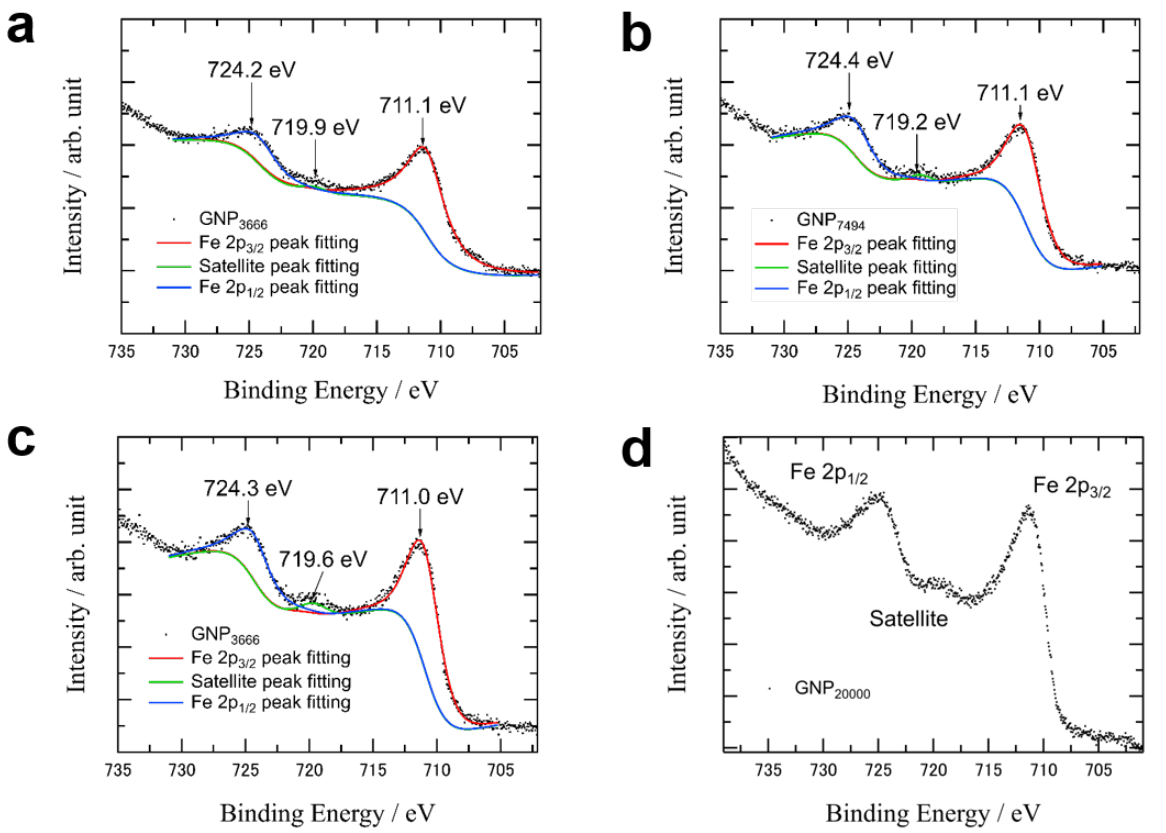

e

Sample	$2p_{3/2}$ / eV	$2p_{1/2}$ / eV	2p satellite / eV
GNP_{3666}	711.1	724.2	719.9
GNP_{7494}	711.1	724.4	719.2
GNP_{18409}	711.0	724.3	719.6

Figure S5. XPS spectra of a) GNP_{3666}, b) GNP_{7494}, and c) GNP_{18409}. d) Multiple components of Fe $2p_{3/2}$ in GNP_{20000} were assigned as 710.11, 710.82, 711.87 and 713.21 eV. e) Summary of the binding energy parameters of GNP_{7494}, GNP_{10900}, and GNP_{18409} at the peak top.

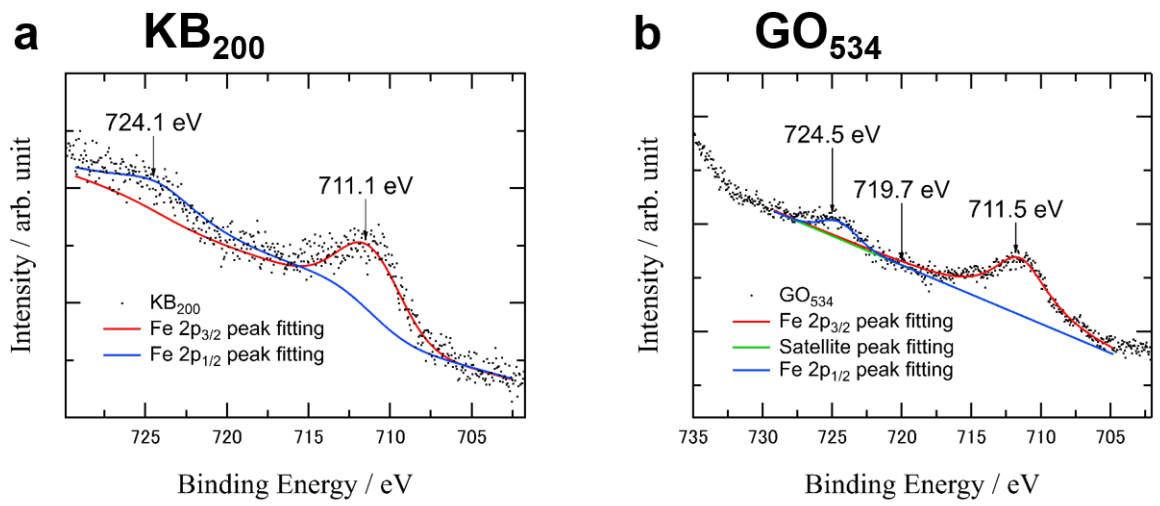

c

Sample	**$2p_{3/2}$ / eV**	**$2p_{1/2}$ / eV**	**2p satellite / eV**
KB_{200}	711.1	724.1	N/A
GO_{534}	711.5	724.5	719.7

Figure S6. XPS analysis of a) KB_{200} and b) GO_{534}. c) Summary of the binding energy of KB_{200} and GO_{534} at the peak top.

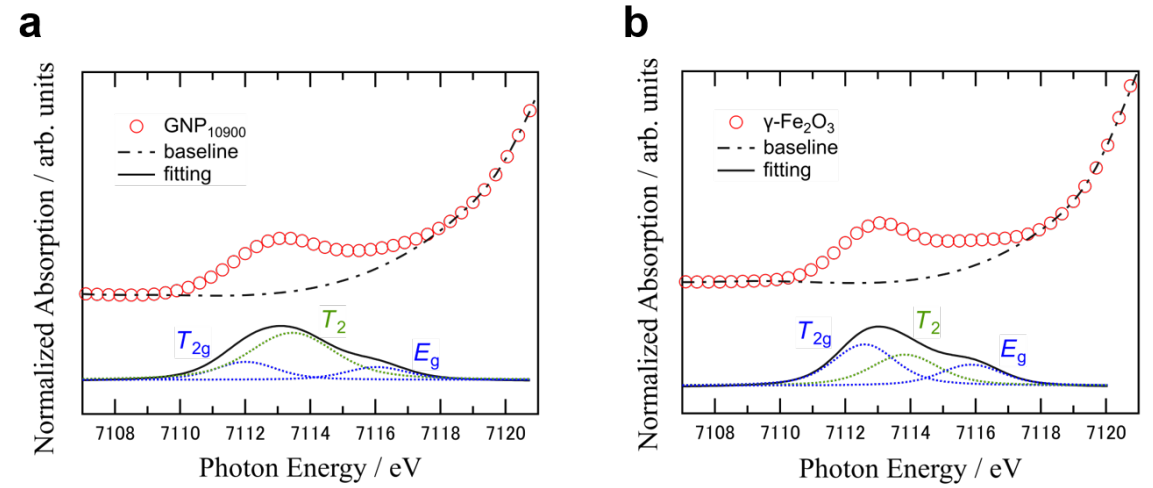

c

Sample	T_{2g}			T_2			E_g			Ratio of T_g/O_h
	Peak energy (eV)	Peak intensity	Integrated area	Peak energy (eV)	Peak intensity	Integrated area	Peak energy (eV)	Peak intensity	Integrated area	
GNP_{10900}	7112.0	0.010497	0.030	7113.4	0.027491	0.107	7116.0	0.0074473	0.021	0.67
γ-Fe_2O_3	7112.6	0.044553	0.128	7113.8	0.033482	0.104	7115.9	0.0226520	0.065	0.35

Figure S7. The Fe K-edge pre-edge region of a) GNP_{10900} and b) γ-Fe_2O_3. These figures display the experimental data (red circles), the baseline, i.e. background function (broken line), a fitting curve to the data (black solid line), and the individual pre-edge peaks for T_{2g}, E_g (blue dotted lines), and T_2 (green dotted line). The fixed FWHM (full width at half maximum) of GNP_{10900} and γ-Fe_2O_3 are as follows. The FWHM values of identical T_{2g} and E_g are 2.242 for GNP_{10900} and 2.242 for γ-Fe_2O_3, that of T_2 is 3.052 for GNP_{10900} and 2.414 for γ-Fe_2O_3. c) List of the obtained parameters of a) and b).

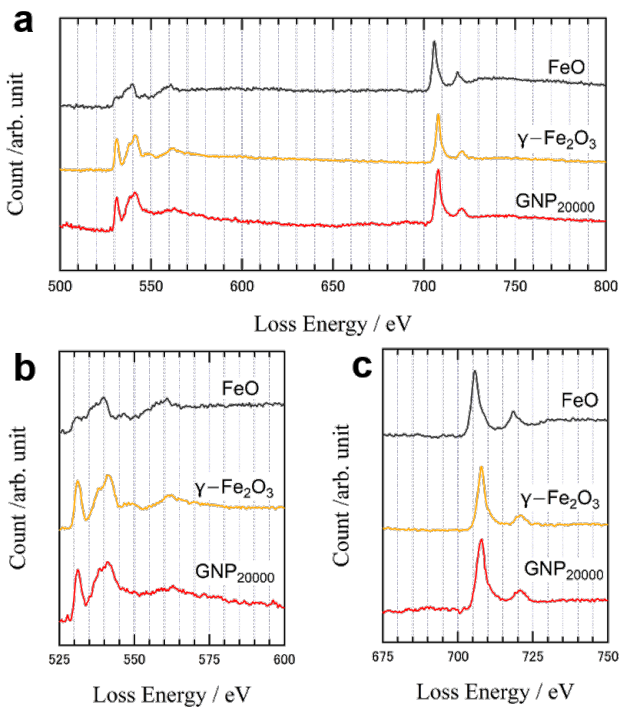

Figure S8. a) STEM-EELS spectra of GNP_{20000} and the standard samples of FeO and γ-Fe_2O_3 for references. The spectra of b) O K-edge and c) Fe L2,3-edge.

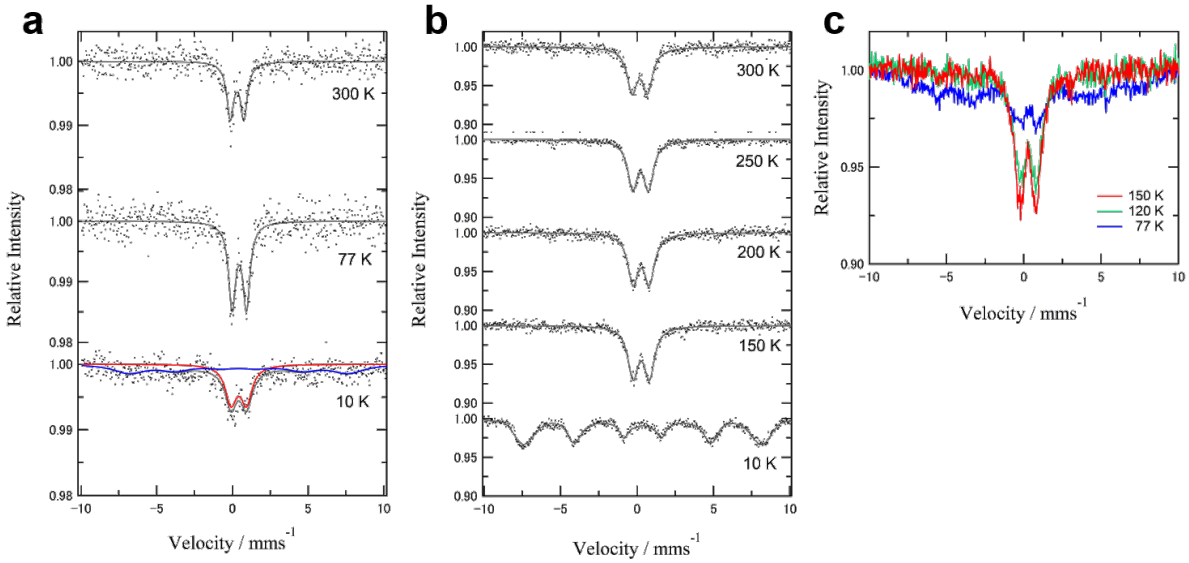

Figure S9. Mössbauer spectra of a) GNP_{3666} and b,c) GNP_{20000} in the temperature range between 300 and 10 K. a) The spectrum of GNP_{3666} at 10 K contained a paramagnetic (red) and a magnetic (blue) components. b) The spectrum of GNP_{20000} at 10 K existed only the magnetic component, and the overlaid spectrum of the temperature change of c) suggests that a magnetic transition temperature exists between 120 and 150 K.

Table S2. Obtained parameters of ^{57}Fe Mössbauer spectra measured for GNP_{3666}, GNP_{10900}, and GNP_{20000}.

Sample	Temp (K)	Paramagnetic (doublet)				Magnetic (sextet)				
		Fraction	IS (mm/s)	QS (mm/s)	LW (mm/s)	Fraction	IS (mm/s)	QS (mm/s)	H_{int} (T)	LW (mm/s)
GNP_{3666}	300	100%	0.309±0.014	0.90±0.02	0.56±0.04					
	10	43.8%	0.42±0.02	1.02±0.04	0.90±0.07	56.2%	0.42±0.02	0	45.0±1.2	2.5±0.7
GNP_{10900}	300	100%	0.346±0.009	0.850±0.015	0.60±0.02					
	10	14.5%	0.494±0.017	0.79±0.04	0.6682±0.0017	85.5%	0.494±0.017	0	40.08 (avg)	0.68±0.09
GNP_{20000}	300	100%	0.180±0.008	1.012±0.013	0.81±0.02					
	250	100%	0.231±0.005	1.038±0.009	0.779±0.015					
	200	100%	0.267±0.007	1.063±0.011	0.818±0.018					
	150	100%	0.268±0.006	1.072±0.011	0.818±0.017					
	10					100.0%	0.364±0.007	0	44.4 (avg)	0.64±0.04

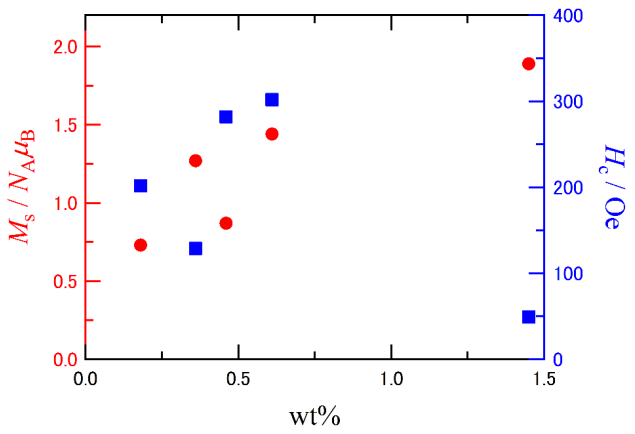

Figure S10. Plots of the saturation magnetization (M_s) and coercivity (H_c) of the GNP_{nn} series against the Fe loading weight (wt%).

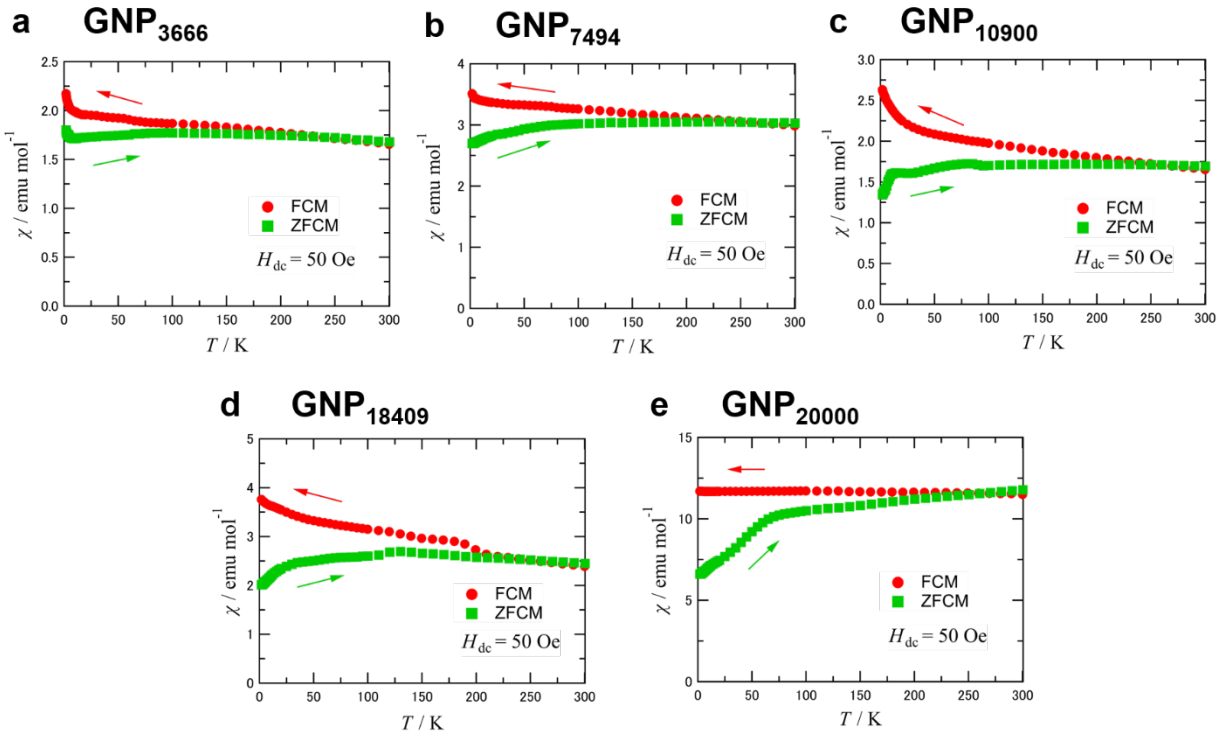

Figure S11. Temperature dependent magnetization of a) GNP_{3666}, b) GNP_{7494}, c) GNP_{10900}, d) GNP_{18409} and d) GNP_{20000}. The red filled circle and green filled square denote field-cooled (FCM) and zero-field-cooled (ZFCM) magnetization, respectively.

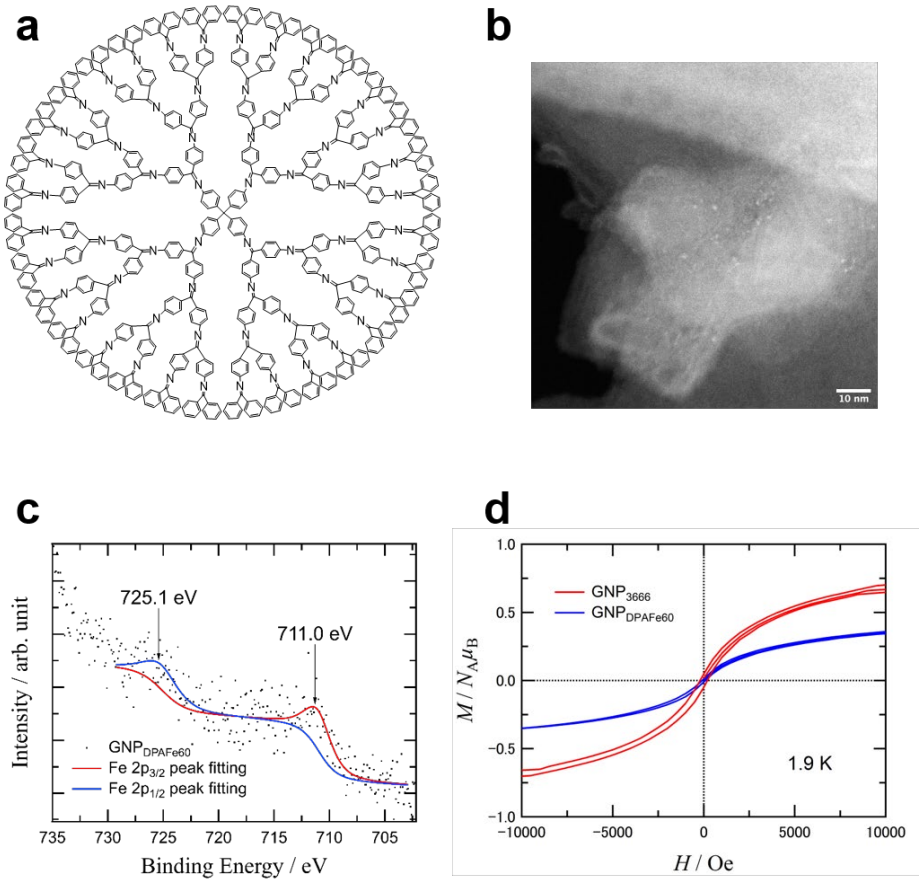

Figure S12. a) Molecular structure of a fourth generation dendritic phenylazomethine template (DPA G4). b) A HAADF-STEM image of GNP_{Fe60} (Particle size = 1.4 nm). c) XPS spectrum of GNP_{Fe60}. d) Magnetization curves of GNP_{Fe60} (blue: 0.41 μ_B) and GNP_{3666} (red: 0.73 μ_B) measured at 1.9 K.